# Observations of Supergradient Winds in the Tropical Cyclone Boundary Layer

Shannon L. McElhinney and Michael M. Bell University of Hawaii at Manoa

Recent studies have highlighted the importance of boundary layer dynamics in tropical cyclone (TC) intensification and structure change. TC boundary layer (TCBL) phenomena such as turbulent kinetic energy, horizontal rolls, momentum fluxes, and gradient wind imbalance are important for TC evolution. However, kinematic fields with adequate spatial resolution to resolve TCBL features are difficult to obtain due to limitations in our observation capabilities.

A TCBL feature of particular interest is the supergradient jet at the top of the boundary layer (Kepert and Wang 2001) associated with boundary layer convergence and forcing of deep convection. The supergradient jet may play a critical role in the formation of eyewalls and secondary eyewalls (Huang et al. 2012). Supergradient winds typically occur only near the inner core where the tangential wind profile is peaked, and when the inward advection of angular momentum exceeds the rate at which it is lost to the sea surface. The local pressure gradient imbalance results in an outward acceleration, which decreases inflow and causes convergence in the TCBL. The low-level convergence and upward motion helps to enhance convection (Kepert and Wang 2001). The existence of supergradient winds has been shown in several observational studies (e.g. Kepert 2006, Bell et al. 2012a, Sanger et al. 2013), but the degree to which the winds exceed gradient balance is still unresolved. It is important to determine the magnitude of the supergradient jet concretely through observations to improve our understanding of TC intensification and eyewall formation.

Airborne Doppler radar can provide some of the highest resolution wind measurements near the top of the TCBL, but the data quality is degraded near the sea surface. Dropsondes, in situ flight-level data, and Stepped Frequency Microwave Radiometers (SFMR) can provide near surface wind information in the TCBL, but also have their own limitations. An improved methodology to retrieve high-resolution low-level TC winds from multiple data sources using a new spline-based, 3-D variational analysis technique called SAMURAI (Spline Analysis at Mesoscale Utilizing Radar and Aircraft Instrumentation) has been developed. The TCBL wind retrieval is similar to that described in Lorsolo et al. (2010) in that it is performed in a "wedge" below the aircraft. However, the SAMURAI variational analysis is performed directly in cylindrical coordinates centered on the TC circulation, and can supplement Doppler radar data with SFMR, flight-level, and dropsonde observations to take advantage of multiple observations. The improved analysis methodology was developed to try and obtain reliable wind fields as close to the surface as possible. It will also be used here to get the pressure gradient field below the aircraft.

To test the methodology, synthetic data was generated from a Weather Research and Forecast (WRF) simulation of Hurricane Rita (2005). The 84-hour simulation consisted of a quadruply nested domain down to 666.7 meters. An idealized figure-four flight track was flown through the simulated storm with an idealized airborne Doppler radar. The radar geometry has similar characteristics to existing tail Doppler radars, but with a simple point beam, no noise, and a flat ocean surface. Several different test cases were run to retrieve the low-level winds using the simulated airborne radar, and a combination of other observations, shown in Table 1. The synthetic radar observations were synthesized using SAMURAI for the "test" run. Perfect in situ wind observations from the model were also analyzed using SAMURAI for the "truth" run. The resulting outputs were then compared to

see how accurate the methodology could be given perfect airborne radar observations. The analyses had no variation in the azimuthal direction in order to determine the optimal width of the wedge.

The value of adding in situ observations in the variational solution was also tested. Synthetic dropsonde observations were created from the model data and added to the SAMURAI input. A dropsonde spacing of 1, 2, 4, 6, and 8 km each were tested. Flight-level observations were also created from the model data at 1.5 km height, to match the flight altitude an initial real data test case. While including SFMR observations is also desired, the best way to use SFMR measurements is still being tested.

**Table 1 RMSE values for the U and V components of each test. The error shows the difference between the test and the truth SAMURAI analysis.**

| Dtheta (degrees) | | | | | Radar | Dropsondes (km) | | | | | Flight-level | Error (m/s) | |
|---|---|---|---|---|---|---|---|---|---|---|---|---|---|
| 5 | 10 | 15 | 20 | 25 | Synthetic | 1 | 2 | 4 | 6 | 8 | 1.5 km | RMSE V | RMSE U |
| | | | | x | x | | | | | | | 2.72 | 1.46 |
| | | | x | | x | | | | | | | 4.31 | 1.74 |
| | | x | | | x | | | | | | | 8.14 | 2.31 |
| | x | | | | x | | | | | | | 12.37 | 3.37 |
| x | | | | | x | | | | | | | 18.42 | 5.48 |
| | | | | x | x | x | | | | | | 2.41 | 0.96 |
| | | | | x | x | | x | | | | | 2.36 | 0.86 |
| | | | | x | x | | | x | | | | 2.34 | 0.93 |
| | | | | x | x | | | | x | | | 2.34 | 1.03 |
| | | | | x | x | | | | | x | | 2.40 | 1.10 |
| | | | | x | x | | | | | | x | 2.35 | 1.39 |
| | | | | x | x | x | | | | | x | 2.31 | 0.93 |

Table 1 shows the results of the different tests of the methodology as RMSE values between the modeled and retrieved winds averaged over all heights and from a radius of 20 to 50 km. Inwards of 20 km there may not be enough hydrometeors for accurate radar wind retrievals, and the cylindrical spatial resolution degrades at larger radii. The rows show the different combinations of observations for retrieving the wind speeds in the V (tangential) and U (radial) directions, and show how much value is added by each observation experiment. For comparison, the RMS values of the wind components are 38.95 $ms^{-1}$ for V, and 3.45 $ms^{-1}$ for U. The tests show that the radar retrieval alone has an RMSE of 2.72 $ms^{-1}$ for V and 1.46 $ms^{-1}$ for U for a azimuthal width of 25 degrees. The RMSE values yield relative errors of 7% for V and 42% for U. Adding flight-level in situ data decreased the error to 2.35 $ms^{-1}$ and 1.39 $ms^{-1}$ respectively. Including dropsonde observations every kilometer was found to improve the V

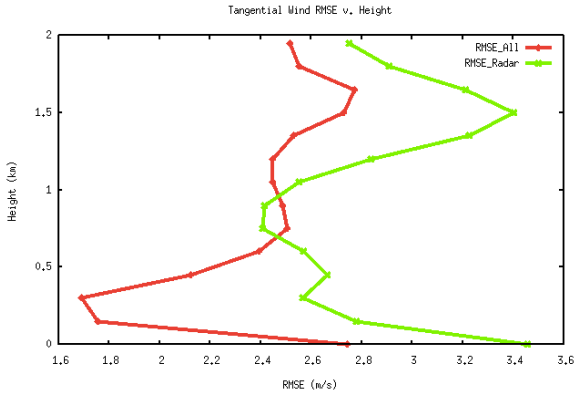


**Figure 1 RMSE with height for V. Green is for the radar data analysis alone. Red is for the analysis with all observations.**

component RMSE to 2.41 $ms^{-1}$ and greatly improve the U component, to 0.96 $ms^{-1}$. When all of the types of observations are used the RMSE is improved to 2.31 $ms^{-1}$ for V and 0.93 $ms^{-1}$ for U. Some of this error may be due to the mass continuity applied to the analysis, which will be turned off in the future for better results.

A paired Student's t-Test was performed for each test to determine if the error reductions were statistically significant. The t-Test paired the mean absolute error (MAE) of the analysis using only radar observations with an azimuthal width of 25 degrees ("control") with the absolute mean error each test. The MAE change for every test was found to be statistically significant at or above the 99% confidence level compared to the control run. The most notable RMSE changes were found by decreasing the azimuthal width of the analysis wedge. The errors increased as the wedge size decreased, suggesting a trade-off between azimuthal spatial resolution and wind accuracy.

Adding dropsonde observations to the analysis significantly improved both V and U in all cases. The relative error reduction was greatest for U, suggesting that dropsondes can provide valuable information to help constrain the under-resolved along- track radar-derived winds (Hildebrand et al. 1996). Adding flight- level in situ observations to the analysis also reduced the errors, and the greatest error reduction was found using radar, dropsondes, and flight level data. The resulting relative errors were reduced to 6% for V and 26% for U. These results suggest that the technique can produce reasonable results with radar-derived winds alone, but incorporating multiple in situ measurements does add significant value to the analysis.

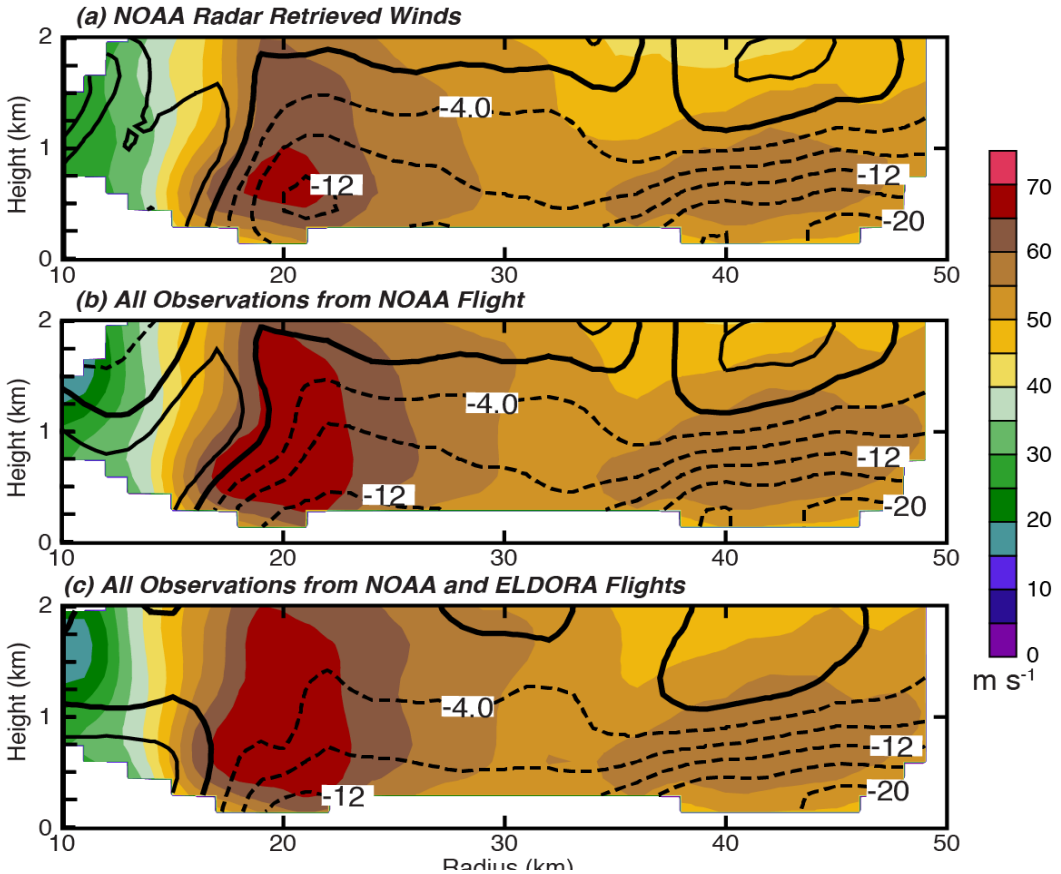


**Figure 2 Tangential wind (color) and radial wind (contour) for Rita on 22 September in the radius height plane. Top panel shows results using NOAA radar observations only, middle panel results using all NOAA observations, and bottom using NOAA and ELDORA.**

Figure 1 shows how close to the surface the winds can accurately be estimated using radar winds alone. It appears that the V wind component can be measured down to 300 m before errors increase, while U (not shown) can be measured down to ~500 m. Including flight-level data in the analysis reduces the error at 1.5 km altitude. The vertical error distribution is promising because supergradient jets and other features of interest are typically within 0.5 and 1.5 km of the surface.

The same methodology was used to test the pressure gradient retrieval, with a few minor changes. Only synthetic dropsonde and flight-level observations are used and the same dropsonde spacing will be tested. The flight-level observations are considered near perfect and in gradient balance at 1.5 km. This pressure gradient is extended to the surface, only changed by dropsonde observations with an increased error. This was done to avoid problems with matching GPS dropsonde heights at different radii. Initial results (not shown) are promising although the error analysis has not been completed.

A real data case using the new methodology was also performed with data from the Hurricane Rainband Intensity Change Experiment (RAINEX) into Hurricane Rita on 22 September 2005. Radar data from the NOAA P-3 tail Doppler radar were edited using a high-threshold automated quality control script in Solo II (Bell et al. 2013). The same tests for azimuthal resolution were performed and the real dropsonde and flight- level observations were added to the Samurai inputs. To further validate the methodology, ELDORA (Electra Doppler Radar) observations and dropsondes from the same time and area were also added to create a "quad-Doppler" analysis that included in situ data. Figure 2 shows the comparison of the wind fields from NOAA radar only, all NOAA observations, and all NOAA and ELDORA observations. The radius-height cross- section in the northern storm quadrant reveals a stronger primary eyewall and weaker secondary eyewall in the V component (color), but with a stronger secondary eyewall and weaker primary eyewall in the U component. These results are consistent with a developing secondary eyewall at this time. The quad-Doppler analysis, which is considered a skillful way to retrieve TC winds, shows good agreement with the analysis using only NOAA observations (see Bell et al. 2012b for comparison).

From the retrieved wind and pressure gradient fields the gradient wind was calculated using the quadratic form of the gradient wind balance equation. The agradient wind was taken as the difference between the retrieved wind and the gradient wind. Where this is positive (negative), supergradient (subgradient) winds are believed to exist. An example of the supergradient wind found at 39 km radius is shown in figure 3 on 22 September as the secondary eyewall was forming. Supergradient wind would be expected here, radially inward of the secondary wind maximum. It is over 10 $ms^{-1}$ supergradient at 600m altitude. A more complete error analysis of the supergradient wind is ongoing.

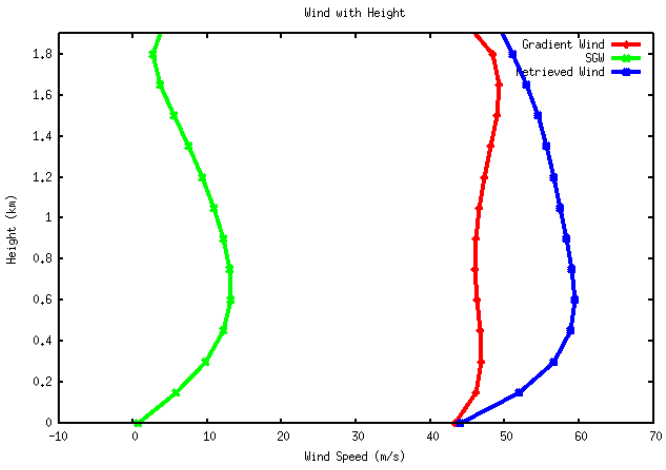


**Figure 3 Supergradient wind (green), gradient wind (red) and retrieved wind (blue) from the SAMURAI analysis of Rita on 9/22 at 39 km radius, using all observations.**

The results demonstrate the ability of the methodology to get a satisfactory wind field for calculating supergradient winds. Initial results for the retrieved pressure gradient field are encouraging, but continued error analysis must be done. The analysis of Hurricane Rita suggest there are supergradient winds in the TCBL just radially inward of the intensifying secondary eyewall. Further quantification of the error for the pressure gradient and supergradient wind will be conducted in the near future.

References

Bell, M. M., M. T. Montgomery, K. A. Emanuel, 2012a: Air–Sea Enthalpy and Momentum Exchange at Major Hurricane Wind Speeds Observed during CBLAST. *J. Atmos. Sci.*, **69**, 3197–3222.

Bell, M. M., M. T. Montgomery, W.-C. Lee, 2012b: An Axisymmetric View of Concentric Eyewall Evolution in Hurricane Rita (2005). *J. Atmos. Sci.*, **69**, 2414–2432.

Hildebrand, P. H., and Coauthors, 1996: The ELDORA/ASTRAIA Airborne Doppler Weather Radar: High-Resolution Observations from TOGA COARE. *Bull. Amer. Meteor.*

Kepert, J. D., Y. Wang (2001). The Dynamics of Boundary Layer Jets within the Tropical Cyclone Core. Part II: Nonlinear Enhancement. *J. Atmos. Sci.*, **58**, 2485–2501.

Kepert, J. D. (2006). Observed boundary layer wind structure and balance in the hurricane core. Part II: Hurricane Mitch. *J. Atmos. Sci.*,, **63**, 2194-2211.

Lorsolo, S., J. A. Zhang, F. D. Marks, and J. Gamache, 2010: Estimation and mapping of hurricane turbulent energy using airborne Doppler measurements. *Mon. Wea. Rev.*, **138**, 3656–3670.

Sanger, N. T., M. T. Montgomery, R. K. Smith, and M. M. Bell, 2013: An observational study of tropical-cyclone spin-up in Supertyphoon Jangmi (2008) from 24 – 27 September. *Mon. Wea. Rev., in press*.